

Car–Parrinello Molecular Dynamics Simulation of Liquid Formic Acid

I. Bakó,^{*,†} J. Hutter,[‡] and G. Pálincás[†]*Chemical Research Center, Hungarian Academy of Sciences, H-1525 Budapest, Hungary, and Physical Chemistry Institute, University of Zurich, CH-8057 Zurich, Switzerland**Received: August 17, 2005; In Final Form: December 15, 2005*

First-principles molecular dynamics has been used to investigate the structural, vibrational, and energetic properties of formic acid, formic acid–formate anion dimers, and liquid formic acid in a periodically repeated box with 32 formic acid molecules. We found that in liquid formic acid the hydrogen-bonded clusters mainly consist of linear branching chains. From our simulation, we got good agreement with the available structural and dynamical data. We also studied the proton transfer in the *cis*-formic acid–formate anion dimer, and we showed that this proton transfer does not have any potential barrier. The hydrogen bonding statistics as well as the mean lifetime of the hydrogen bonds are analyzed.

Introduction

The hydrogen bond is of great interest and importance both as a special type of chemical bond occurring in a wide variety of molecular complexes and also of its pervasive presence in biochemical systems. It largely determines the physical properties of many common condensed-phase systems including water. It represents the strongest force governing the influence of solvents on molecular structure and reactivity. Proton transfer within a hydrogen bond is a fundamental reaction in chemistry, biochemistry, and related fields. Understanding the nature of the hydrogen-bonding interaction is very important. The first step in these processes involves the investigation of small model molecules. Water is the prototype for the study of the hydrogen bond, and for this reason, it has received a great deal of attention from both the theoretical^{1–5} and experimental^{6–10} points of view.

Formic acid, the simplest carboxylic acid, is a compound of special interest in many respects. This molecule can be expected to act as a proton donor and acceptor. The donor characteristic of the formyl hydrogen can appear in unconventional C–H···O-type hydrogen bonds. The complexity of the hydrogen-bonding pattern is manifested in the condensed phase structure of formic acid. In the gas phase, formic acid molecules can form centrosymmetric dimers in which the two molecules are held together by two equivalent hydrogen bonds.¹¹ Recently it was showed by Madeja et al.¹² that, in an ultracold helium nanodroplet, the preferred formation of formic acid dimer is a chainlike, acyclic structure and not the cyclic isomer with two H-bonds. X-ray- and neutron-diffraction studies of crystalline formic acid show that the molecules form a long hydrogen-bonded chainlike structure.^{13,14} The molecular association in the liquid phase has been studied by a wide variety of experimental and theoretical methods.^{15–24} Several infrared¹⁵ and Raman¹⁶ spectroscopic investigations showed the existence of cyclic dimers and the chainlike polymer structure in the liquid state. The X-ray- and neutron diffraction experiments described the structure of liquid formic acid in terms of hydrogen-bonded chains.^{17–20}

The structure of liquid formic acid has already been studied by molecular dynamics (MD), the Monte Carlo (MC) and Reverse MC methods.^{21–24} According to these studies the frequently used optimized potentials for liquid simulations (OPLS) potential parameter set cannot reproduce the structural properties of liquid formic acid. Recently a new five-site pair-potential model was developed for formic acid by fitting to an “ab initio” dimer potential surface.^{23,24} Results from the simulations with this new pair potential showed a better agreement with the experimental structure and thermodynamic data. However, the flexibility and polarizability of the formic acid molecule are not included and neither is the many-body effect.

Prompted by these considerations, we have undertaken an “ab initio” molecular dynamic simulation of liquid formic acid. It has been already shown that this method can be applied to molecular liquids. Liquid water,^{25–27} methanol,²⁸ ammonia,²⁹ hydrogen fluoride,³⁰ dimethylsulfoxide–water mixture,³¹ formate ion hydration,³² and hydration problems of several ions^{33–38} have been already studied by this method. During the period of publication of this work a Car–Parrinello MD (CPMD) simulation was published.³⁹ The authors of that work inferred the importance of heterocyclic dimer configurations in the liquid state, which dimers are embedded into the H-bonded chain. They did not show any dynamical results from the ab initio MD simulation.

Computational Details. The present study was performed by using the ab initio CPMD scheme. The electronic structure was described by density functional theory. Becke’s (B) gradient corrected exchange functional³⁸ and Lee–Yang–Parr’s (LYP) coorelational functional⁴⁰ were used. It has been already shown that the BLYP functional gives a reasonable description of a hydrogen-bonded liquid, similar to water.^{25–27} The valence electronic wave functions are expanded in plane waves with a 70-Ry cutoff, and the valence–core interaction was described by the Troullier–Martins normconserving pseudopotentials.⁴¹

For the calculation of the gas-phase molecules and complexes in the deuterated form, a cubic supercell was used with a cell length chosen to be large enough to prevent the interaction between the periodic images. The effect of the unit cell length was checked by expanding the box size to about 10 Å. Only a minor variation of the total energy (about 0.1 kJ/mol) was found.

* To whom correspondence should be addressed. E-mail: baki@chemres.hu.

[†] Hungarian Academy of Sciences.

[‡] University of Zurich.

TABLE 1: Interaction Energies (kcal/mol) of Different Type of Formic Acid Dimer

HT ^a	II	III	IV	V	VIII
BLYP/a	13.90	7.42	4.45	5.90	2.17
BLYP/TM	14.05	7.92	4.55	6.38	1.80

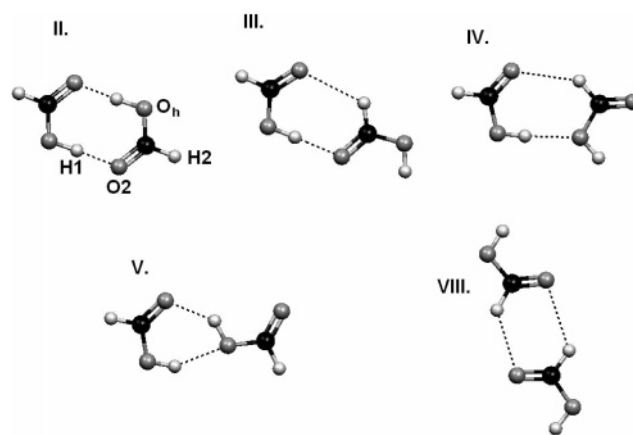
^a a, aug-cc-pVTZ; TM, planewave basis with 70-Ry cutoff energy.

The formic acid–formate anion dimers were investigated as an isolated system in a cubic box using the Martyna–Tuckerman⁴² method to decouple the system from its periodic images with 100-Ry planewave cutoff.

A liquidlike system was made up of $N = 32$ DCOOD molecules enclosed in a cubic box at the experimental density about 1.266 g/cm³. A classical molecular dynamics simulation using the newly developed potential model for liquid formic acid was used to generate the initial configuration. In the initial configuration the formic acid molecule did not have an exact planar configuration. The CPMD⁴² simulation was run using a time step of $\Delta t = 0.144$ fs, and the fictitious electron mass (μ) was 600 au. A continuous trajectory of 7 ps was obtained in the microcanonical ensemble with the last 6 ps used for the computation of average properties. The temperature was set to 300 K. Recently a series of CP and Born–Oppenheimer (BO) molecular dynamic simulations were carried out for liquid water to investigate the reproducibility of this method.^{44–48} They showed that for structural properties size effects are rather small, but care is required in the choice of an appropriate electron mass. It is important in CP simulations to maintain an adiabatic separation between electronic and ionic degrees of freedom. In our case this could be achieved with a mass ratio μ/M (M is the smallest atomic mass of the system) of $1/6$. We did not find any energy drift in our simulation, and the conserved energy fluctuation was about $10^{-7}\%$ (approximately 10^{-4} au).

Gas-Phase Results. a. Monomer. To verify the accuracy of our model, we investigated the *cis*- and *trans*-formic acid molecules and formate anion structure at different levels of theory. The structural data could be found in the Supporting Information. Our calculations showed a close agreement with the BLYP, MP2, and experimental results and establish the validity of the pseudopotentials and density functional employed. The energy difference between the two conformers of formic acid is also in good agreement with high level theoretical calculations.⁵⁰

b. Formic Acid Dimer. It has already been shown that density functional theory (DFT) can provide a reasonable representation of the dimerization process in the gas phase for the formic acid centrosymmetric dimer.^{51–54} Turi has studied the different hydrogen-bonded complexes of formic acid.⁵² We performed geometry optimizations for the five most stable earlier studied bimolecular complexes, and the results are shown in Supporting Information and Table 1. The optimized minimum-energy structures are shown in Figure 1. In this case we use the same notation as in the Turi paper.⁵² The cyclic dimer is denoted by II. III corresponds to an H-bonded complex that can be found in crystal state. From Table 2 it becomes evident that the O–H and C=O bonds in structure II and III are significantly elongated, while C–O bonds are shortened. III, IV, V, and VIII also contain C–H \cdots O-type interactions. Structure VIII can be characterized by two equivalent C–H \cdots O-type interactions. All optimized structures were close to the planar configuration, even if the starting structures were nonplanar. The experimental dimerization energy of centrosymmetric dimer (II) from NMR experiment was about 13.2 kcal/mol.^{55,56} Other high-level ab initio calculations (B3LYP/

**Figure 1.** The five optimized structures of dimers of formic acid. The numbering follows that according to Turi (ref 52).**TABLE 2: Vibrational Frequencies for Investigated Formic Acid Dimers (Data in cm⁻¹, Experimental Value from Refs 15 and 16)**

	monomer	II	III	IV	V	VIII
$\nu(\text{O–H})$						
BLYP/a	2590	2220	2593	2602	2404	2596
			2330	2484	2352	
BLYP/TM	2537	2078	2561	2545	2433	2548
			2298	2444	2352	
Exptl	2631	2068				
$\nu(\text{C–H})$						
BLYP/a	2199	2152	2188	2197	2210	2227
			2243	2242	2188	
BLYP/TM	2214	2224	2189	2220	2208	2240
			2250	2257	2234	
Exptl	2231	2210				

aug-cc-pVTZ, MP2/aug-cc-pVDZ, CCSD(T)/aug-cc-pVDZ)^{51–54} for this dimer gave a dimerization energy between 13.4 and 14.5 kcal/mol. Chelli et al. reported a dimerization energy of about 18.5 kcal/mol using a similar method as we used in our calculations, which is about 30% larger than our result.³⁹ The geometric and energetic data from optimization using a plane-wave basis set are in good agreement with the experimental and other ab initio calculations. The characteristic frequencies of the OH and CH stretching modes in the dimer can be found in Table 2. It can be seen that the OH stretching mode in every case has a red shift and that the CH has a small blue shift compared to the monomer. We can find the most significant red shift of OH stretching frequencies in structure II (458 cm^{-1}). It has already been shown that the anharmonicity also causes a significant red shift in OH stretching frequencies.⁵⁷ This is very clear for the result of dimer VIII, where no OH hydrogen bond can be found. The origin of the blue shift of the C–H frequency in the C–H \cdots O hydrogen bond has already been studied.^{57–59} It was shown that both blue-shifted and red-shifted hydrogen bonds are governed by the same interaction. These data can be interpreted by the increased electron density (ED) on the OH antibonding orbital and the decreased electron density on CH antibonding orbital.

The double proton transfer in the centrosymmetric dimer has already been studied by high-level quantum chemical calculations and CP simulations as well.^{61–63}

c. Formic Acid–Formate Anion Dimer. The proton transfer is one of the simplest and most fundamental steps in many chemical and biological reactions. This transfer through hydrogen bonding is an important mechanism by which many chemical and biological processes are carried out. These processes have already been studied in the *cis*-formic acid–

TABLE 3: Characteristic Properties of Formic Acid–Formate Anion System (Distance in Angstroms, Energy in kcal/mol)

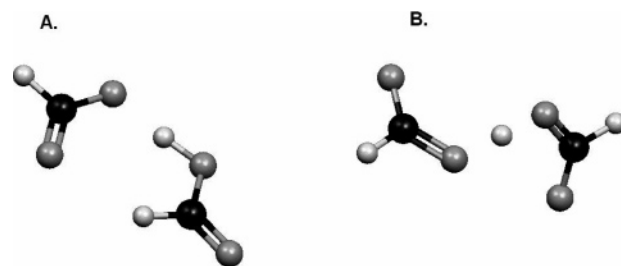
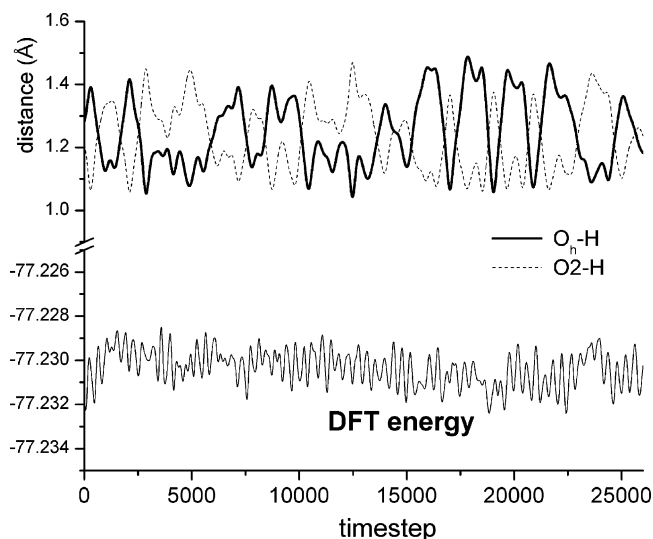
<i>trans</i> -Formic Acid–Formate Anion		
	BLYP/a	100 _{TM}
OCO	129.4	128.77 (128.9)
O···H	1.23	1.33 (1.298)
C–O _h	1.3018, 1.23	1.299, 1.242
C=O ₂	1.30, 1.23	1.31, 1.236
O ₁ –H	1.23	1.14 (1.165)
O···O	2.45	2.46 (2.45)
–ΔE	26.9	23.2 (24.5)
<i>cis</i> -Formic Acid–Formate Anion		
	BLYP/a	BLYP/TM
OCO	128.4	123.86, 128.4
O···H	1.47	1.482
C–O _h	1.321, 1.231	1.332, 1.251
C=O ₂	1.249, 1.286	1.2308, 1.288
O _h –H	1.07	1.062
O···O	2.53	2.54
–ΔE	33.41	31.01

formate anion system using three different theoretical methods (MP2, BLYP, and B3LYP) with a medium-sized basis set.^{60,61} The results show that the DFT method describes correctly the energetic and geometric behavior of this type of systems. The total energy varies in a very narrow range, suggesting a very small energy barrier for the proton transfer. In our calculation we investigated the *cis*-formic acid–formate anion and *trans*-formic acid–formate anion system using DFT/BLYP method with a larger basis set (aug-cc-pVTZ) and planewave basis set with 100 Ry. The calculated energetic and geometric results for both studied systems can be found in Table 3, and the structures of these systems are shown in Figure 2.

trans-Formic acid has a higher binding energy to the formate anion than the *cis* conformer according to both calculations (33.4 and 31.0 kcal/mol respectively). The two methods give very similar results, but the interaction energy in both complexes is higher using localized basis sets. According to these results, both complexes have a very short hydrogen bond. The stability of the system, calculated using a planewave basis set, was investigated using an ab initio molecular dynamics method at 100 K. The *trans*-formic acid–formate anion system was found as a stable configuration. The potential energy and the O_h–H, and O₂–H (O_h, alcoholic oxygen; O₂, carboxylic oxygen) distances as a function of time is shown in Figure 3 for the *cis*-formic acid–formate anion case. This corresponds to the process of proton transfer from the formic acid molecule to formate anion. It can be seen from Figure 3 that the proton does not have any potential barrier along the reaction path.

Partial Pair Correlation Function for Liquid Phase. According to our calculations, the intramolecular geometry of formic acid molecule in the liquid phase is similar to the gas-phase geometry. The CO₂ and OH bond elongated by about 0.02 Å, and the CO_h bond shortened by about 0.01 Å. All of the molecules in our simulation box were nearly in planar configuration during the simulation, which is in good agreement with our previously published neutron diffraction results¹⁹ but did not support the results of Bertagnoli et al.¹⁸ The partial pair correlation functions calculated from the CPMD simulation are presented in Figure 4. Results of an analysis of the classical MC simulation²² are also shown in comparison. The characteristic value of the partial radial distribution functions are found in Table 4.

The existence of the hydrogen-bonding nature of this liquid is clearly indicated by the very well defined peak of $g_{O_2H_1}$ (H1,

**Figure 2.** The optimized structure of formic acid–formate anion dimer (A, *trans*-formic acid–formate anion; B, *cis*-formic acid–formate anion).**Figure 3.** Change of total energy and O_h···H and O₂···H distances during the proton transfer in *cis*-formic acid–formate anion dimer.

alcoholic hydrogen) at 1.7 Å. Integration of this peak, up to the first minima at 2.45 Å, results in a coordination number of 0.92. This value is in good agreement with the coordination number from classical simulation, however the peak position shifts by about 0.05 Å to a smaller distance. The O_h–H₁ peak is smaller, and the coordination number of this peak is also smaller than the classical simulation, so the O_h–H₁···O_h-like hydrogen bonds are very rare in the investigated system. The $g_{O_2H_2}(r)$ (H₂, formic hydrogen) function exhibits a distinct peak at 2.57 Å, and the coordination number is 1.6 if the integration is carried out up to 3.5 Å. The position of this peak is also comparable with the H₂···O₂ distance of C–H₂···O hydrogen bonds in crystalline formic acid.

The CC, CO₁, and CO₂ partial pair correlation functions are in good agreement with the previous MC and RMC results.^{21,23} The integration numbers of these partial pair correlation functions up to the first minimum are 12.4, 12.0, and 11.8, respectively. The radial distribution functions calculated from our simulation look very similar to those presented in earlier ab initio MD work.³⁹

Geometry of Hydrogen Bonds. A plot of the hydrogen-bond angular distribution of the O–H–O and C–H···O angles is given in Figure 5. The O_h–H₁–O₂ and C–H₂–O₂ cosine angle distributions have an average value of 152.8 and 124.7°, respectively. Clearly the most favored arrangement of the two hydrogen bonded molecules in the O_hH₁O₂ case corresponds to a linear hydrogen bond. This behavior cannot be seen on the CH₂O₂ cosine angle distribution, as the bonds deviate much more from the linear hydrogen bond than the O_hH₁O₂ bond. The integration of the distribution functions indicates that φ is larger than 130° in 90% of the hydrogen bonds. The corre-

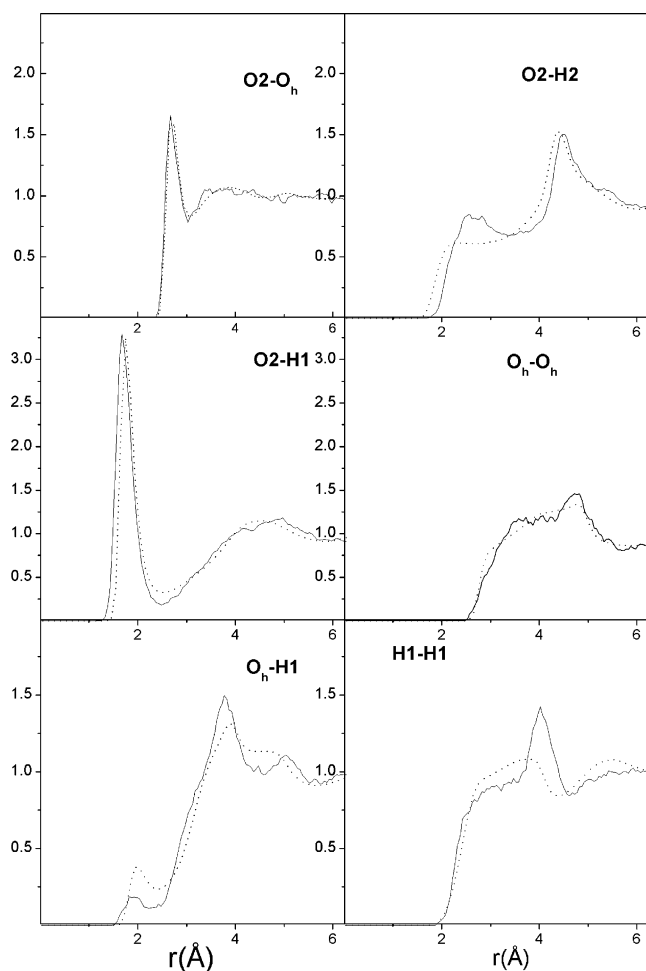


Figure 4. Set of site-site radial distribution functions for formic acid from CPMD and MC calculations (line, CPMD; dashed, MC).

TABLE 4: Characteristic Parts of the Intermolecular Parts of Site-Site Radial Distribution Functions for Liquid Formic Acid^a

	r_{\max}	$g(r_{\max})$	r_{\min}	$g(r_{\min})$	$N(r_{\max})$	$N(r_{\min})$
CC	4.32	2.01	5.7	0.69	4.7	12.4
CO ₂	3.42	1.77	4.22	1.03	1.27	4.22
CH _o	2.575	1.11	3.18	0.57	0.31	1.08
O ₂ O ₂	3.42	1.85	5.02	0.81	1.36	7.60
O ₂ O ₁	2.67	1.65	3.23	0.88	0.36	1.91
O ₂ H _o	1.68	3.29	2.42	0.21	0.29	0.90
O ₂ H ₂	2.57	0.84	3.47	0.68	0.42	1.66
O _h H _o	1.92	0.18	2.37	0.11	0.01	0.1

^a r_{\max} , peak position; $g(r_{\max})$, peak height; r_{\min} , minimum position; $N(r_{\min})$, coordination number; distances are in angstroms.

sponding value for the C-H₂...O₂ interaction is 45%. We also calculated the cosine distribution of another angle characterizing the hydrogen bonds, namely, the angle between the O-H or C-H and the OCO plane of acceptor molecule (Figure 5). These distributions characterize the planarity of the hydrogen bond. It is apparent from the cosine distribution that the planarity is fulfilled much better than the linearity of the hydrogen bond.

Molecular Cluster Analysis. To study the molecular clusters in liquid formic acid we apply the formalism of Geiger,⁶⁴ which was originally applied to liquid water. In this treatment a cluster is defined as a group of molecules among which any two are connected to each other by a chain of hydrogen bonds. A geometric criterion similar to that considered in the classical molecular dynamics study was used for the definition of the

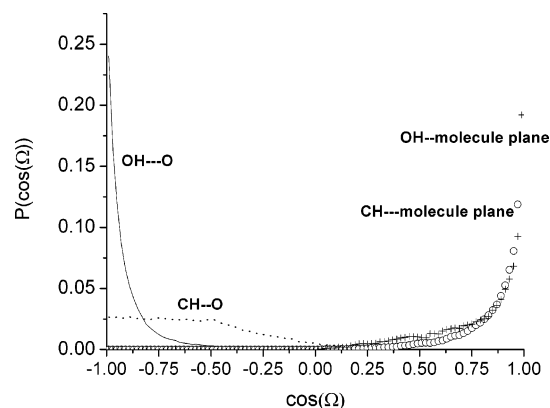


Figure 5. Cosine distribution of three hydrogen bond angles characterizing the geometry of hydrogen bonds: O_hH...O₂ (solid line) and CH...O₂ (dashed line) angle, angle between the OH bond and acceptor molecule plane (dotted line), and angle between the CH bond and acceptor molecule plane (star).

TABLE 5: Statistical Properties of the Hydrogen Bonded Networks in Liquid Formic Acid Using the Geometric Hydrogen Bond Definition^a

α^b	f_0	f_1	f_2	f_3	f_4
100	0.014	0.21	0.53	0.21	0.02
130	0.025	0.23	0.57	0.15	0.01
	(0.02)	(0.265)	(0.558)	(0.142)	(0.01)
150	0.099	0.358	0.457	0.083	0.00

	n_{hb}	N	M	n_g	M_g	n_c	M_c
100	2.01	8.48	3.77	9.54	3.3	4.88	2.9
130	1.87	6.45	4.95	7.54	4.12	2.93	2.9
	(1.85)						
150	1.57	3.28	9.75	4.35	6.57	0.16	

α^c	f_0	f_1	f_2	f_3	f_4	n_{hb}	n	n_g
130	0.409	0.451	0.12	0.023	0.015	0.77	1.63	2.81

α^d	f_0	F_1	f_2	f_3	f_4	n_{hb}	n	n_g
130	0.008	0.098	0.442	0.354	0.087	2.43	28.71	29.05

^a f_n , fraction of the molecule having exactly n hydrogen bonds; n_{hb} , average hydrogen bond number; n , average cluster size; n_g , average gel cluster size; n_c , average cyclic structure size; m , average cluster number; m_g , average gel cluster number; m_c , average cyclic structure number. ^b Hydrogen-bond definition: O₂-H_o, O_h-H_o < 2.5 Å and OHO > α . ^c Hydrogen-bond definition: C-H₂...O < 2.5 Å and CHO > α . ^d Hydrogen-bond definition: O₂-H_o, O_h-H_o < 2.5 Å and OHO > α and C-H₂...O < 2.5 Å and CHO > α .

hydrogen bonds in liquid formic acid. According to this definition an intermolecular hydrogen bond exists between two molecules if the H₁-O₂ or H₁-O_h distance is smaller than 2.5 Å and the O-H-O angle is smaller than an arbitrary φ_c value. These two constraints were chosen to guarantee that the analyzed pairs were truly hydrogen bonded. The specific distance was based on the first minimum on the O-H radial distribution function. Table 6 summarizes the calculated statistical properties at three different values of φ_c . In this table f_i is the fraction of molecules having exactly i hydrogen-bonded neighbors, n_{hb} is the average number of hydrogen bonds in which a molecule participates. The size of a cluster n simply defines the number of molecules belonging to it. The clusters containing more than one molecule are called gel cluster and are denoted by n_g . The number of different type of clusters (cluster, gel cluster) are called M and M_g respectively. We denoted a cluster as cyclic if we start from one of the molecules of the cluster and going along intact hydrogen bonds we go back to the same molecule.

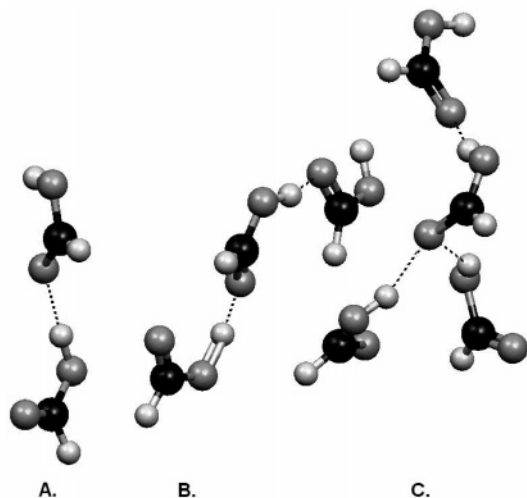


Figure 6. Selected configuration of H-bonded formic acid cluster from simulation.

The average cluster or gel cluster size is still below 10 when the hydrogen bonds are defined with the most permissive definition ($\varphi_c = 100^\circ$). The average cyclic cluster size is about 3. According to our calculation the fraction of molecule incorporated in centrosymmetric cyclic dimer structure (dimer II) was about 12–14% of the total number of formic acid molecules in the simulation box. This value is about 10% smaller than the value reported by Chelli et al.³⁹ in earlier ab initio MD work. This difference can be explained by the difference of the strengths of the hydrogen bonds in dimer II, which was reported to be about 30% stronger in the earlier ab initio MD work. A more reasonable limiting angle ($\varphi_c = 130^\circ$), which is the same as was applied in the earlier MC calculation, shows that the chain often has branch points. With this definition about 15% of the molecules are in a branched position participating in at least three hydrogen bonds. A few examples of the various types of molecular clusters found in the configurations obtained from the simulations are shown in Figure 6.

To obtain comparable results with Turi et al., we also calculated the characteristic values of the hydrogen bonded network, for both type of hydrogen bond, namely $\text{OH}\cdots\text{O}$ and $\text{CH}\cdots\text{O}$. In Table 5, we show these data. It can be seen that in the liquid formic acid the molecules form a space-filling network. The same was concluded by Turi et al. MC and Chelli et al. ab initio MD work.

Comparison of CPMD Results with the Neutron-Diffraction Data. Several neutron and X-ray diffraction experiments on liquid formic acid can be found in the literature.^{17–21} A detailed study by Bertagnolli et al.^{17,18} has shown that formic acid in the liquid state is a molecule for which the OH group is rotated by about 50° from the molecular plane. Other results do not agree with this conclusion.^{19,21} In these studies H/D isotopic substitution was applied to obtain three different partial pair correlation functions (RR, RH, HH, where R is the HCOO group of the formic acid molecule). The distinct RDF, which is characteristic for the liquid structure and does not include the intramolecular contribution, has been calculated from the partial site–site radial distribution functions according to the equation

$$G(r) = \frac{(2 - \delta_{\alpha\beta})x_\alpha x_\beta b_\alpha b_\beta g_{\alpha\beta}(r)}{\left(\sum_\alpha x_\alpha b_\alpha\right)^2}$$

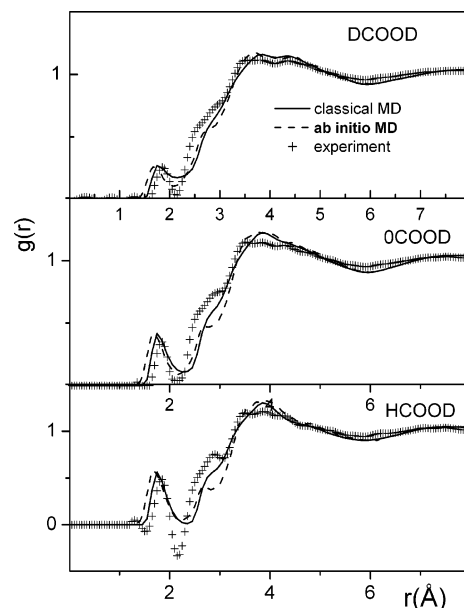


Figure 7. The total intermolecular radial distribution function for liquid formic acid from CPMD and molecular dynamics simulation and neutron diffraction measurement on different isotopic composition. (a) DCOOD, (b) D/HCOOD, (c) HCOOD. D/H: the average scattering length of this site is 0. (Experimental data is from ref 19.)

where b_α is the scattering length of the α particle and x_α is the mole fraction of the α particle.

The experimental¹⁹ and calculated $G(r)$ values for different isotopic compositions are compared in Figure 7. The first peak on the experimental $G(r)$ which is at around 1.85 \AA can be assigned to the distance of the $\text{O}\cdots\text{H}$ hydrogen bond. The second shoulder or small peak at around $2.7\text{--}2.8 \text{ \AA}$ contains contribution from $\text{O}_h\text{--O}_2$ but also from C--H_2 , $\text{O}_2\text{--H}_2$, and $\text{H}_1\text{--H}_1$ because the scattering length of deuterium is in the same magnitude than that of carbon and oxygen ($b_D = 0.667 \text{ fm}$, $b_C = 0.664 \text{ fm}$, $b_O = 0.583 \text{ fm}$). It is shown that all qualitative features of the experimental curve are well reproduced by the CPMD and the new classical MD²⁴ calculation.

Dynamical Properties. The self-diffusion coefficient is a sensitive indicator of the accuracy of the applied model. The self-diffusion coefficient was estimated from the Einstein relation, which uses the long time limit of the mean square displacements of the center of mass of the molecule. The value predicted from the simulation is about $1.26 \times 10^{-5} \text{ cm}^2/\text{s}$, which is about 20% higher than the experimental value for pure HCOOD liquid at 293 K ($1.04 \times 10^{-5} \text{ cm}^2/\text{s}$).⁶⁵ Because the average displacement over 6 ps is similar in magnitude to the molecular diameter, this value from the simulation can depend on the simulation length and size; therefore the good agreement between theoretical and experimental value has to be considered fortuitous.⁴⁷

The vibrational spectra of hydrogen-bonded systems are an important source of information on the hydrogen bonding. These spectra can be obtained directly by the Fourier transformation of the individual atomic velocity autocorrelation functions without any correction to the drag from the fictitious electron mass.⁴⁵ In our case this correction factor depends slightly on the vibration mode and the correction term is in the range of 1.03–1.06. The computed spectral densities, which are calculated directly from the Fourier transformation of the velocity autocorrelation function of formyl and acetic H, are shown in Figure 8. The O_hH_1 and CH_2 stretching frequencies in the gaseous state of formic acid molecule are 2537 and 2214 cm^{-1} .

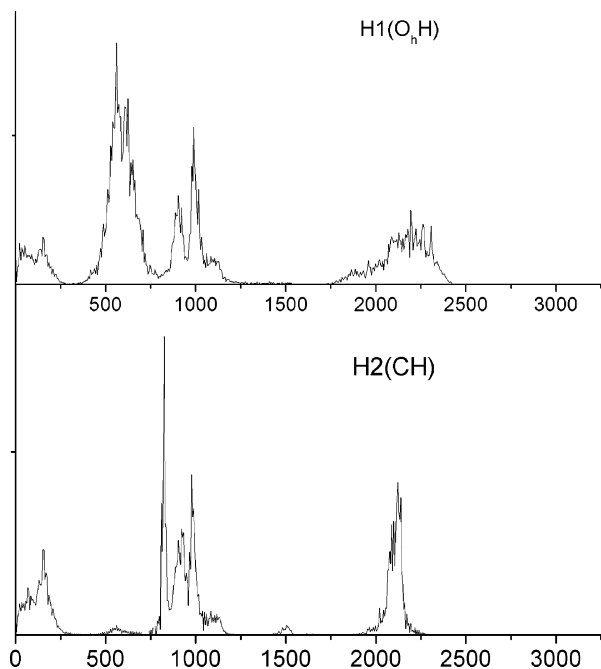


Figure 8. The spectral densities of acetic and formic hydrogen of formic acid calculated from velocity autocorrelation function of these hydrogens.

The corresponding frequencies for the optimized dimers are found in Table 2. We could not detect any important contribution around 2400–2600 cm^{-1} in the spectra. We can conclude that almost all of the acetic hydrogens are involved in hydrogen bonds. The maximum height position in the $\text{O}_h\text{H1}$ spectra is at about 2180–2190 cm^{-1} (the corrected value is about 2290–2300 cm^{-1}). These data correspond to our finding about the structure of liquid formic acid, which has a branching chainlike structure. There is some hint in the spectra below 2000 cm^{-1} (the corrected value is about 2100 cm^{-1}) pointing to strong hydrogen bonds.

The reorientation process in the system can be described by the orientational correlation function $C_1(t)$, which is defined in the following way

$$C_1(t) = \langle P_1(\cos(\Theta(0)))P_1(\cos(\Theta(t))) \rangle$$

where P_1 is a Legendre polynomial and $\theta(t)$ is the angle through which a molecular fixed vector rotates in a time t . The $\text{O}_h\text{H1}$ vector is of particular interest here, since the correlation time of the second member of the series (τ_2) from eq 2 is related to the spin–lattice relaxation time measured by the NMR experiments. The experimental value for τ_2 is between 4.2 and 6.5 ps.^{65,66} The corresponding $C_1^{\text{OH1}}(t)$ and $C_2^{\text{OH1}}(t)$ are shown in Figure 9. Our computed relaxation time of 5.07 ps is in a good agreement with the experimental value. For comparison, the classical OPLS simulation of liquid formic acid gives a value of about 12.5 ps, considerably higher than than the experimental value.

In addition to the H-bond static properties, we calculated the survival probability or lifetime of the H-bonds in a similar way to Rapaport⁶⁷ and Starr et al.⁶⁸ In these works the definition of H-bond lifetime based on the time correlation function $[C(t)]$. In these correlation functions the dynamical variable is 1 if the molecule pair is connected by hydrogen bond and zero otherwise. The resulting $C(t)$ functions with different angle criteria are shown in Figure 10. It is clear from this figure that the $C(t)$ functions decay exponentially at large times ($t >$

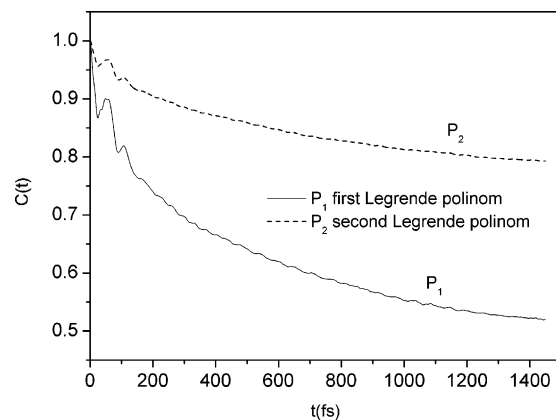


Figure 9. Reorientational time correlation function for the O–H bond direction.

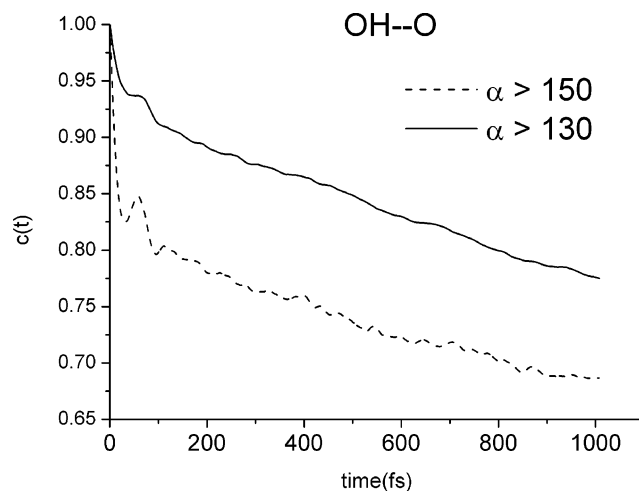


Figure 10. H-bond lifetime autocorrelation function for formic acid (solid, $\text{O}\cdots\text{H} < 2.5 \text{ \AA}$ and $\text{OH}\cdots\text{O} > 130$; dotted, $\text{O}\cdots\text{H} < 2.5 \text{ \AA}$ and $\text{OH}\cdots\text{O} > 150$).

0.2 ps). The H-bond lifetime obtained by this method is about 4.5–5.5 ps. For liquid ethanol, which has similar H-bonded pattern, the H-bond lifetime using the same method was about 3.5 ps.^{69,70} For $t < 0.2$ ps, $C(t)$ decays rapidly due to the librational motion, and this decay depends largely on the H-bond criteria.

Summary

We have performed gas-phase DFT and planewave CPMD calculations on formic acid and formic acid–formate anion dimers and CPMD simulations on liquid formic acid using a periodic box of 32 formic acid molecules. We found that for the stable formic acid and formic acid dimers the two methods give nearly the same energetic and structural results. We also showed that the proton transfer in the *cis*-formic acid–formate anion system is almost barrierless. We observed a good agreement with the recent neutron scattering experiment.¹⁹ The comparison with experimental dynamical properties for liquid formic acid also shows a general agreement. Analysis of the hydrogen-bonded clusters revealed that the liquid phase consists of short branching chains, where the molecules are connected by $\text{OH}\cdots\text{O}$ hydrogen bonds. We also observed about 12–14% cyclic dimer in our simulation box. The calculated hydrogen bonded lifetime is very close to the calculated lifetime in liquid methanol or ethanol, which have a similar H-bonded pattern.

Supporting Information Available: Geometry optimizations for five bimolecular complexes and results. This material is available free of charge via the Internet at <http://pubs.acs.org>.

References and Notes

- Reed, A.; Curtis, L. A.; Einhold, F. *Chem. Rev.* **1988**, *88*, 899.
- Buckingham, A.; Fowler, P.; Hutson, J. *Chem. Rev.* **1988**, *88*, 963.
- Mishima, O.; Stanley, E. *Nature* **1998**, *392*, 164.
- Luzar, A.; Chandler, D. *Nature* **1996**, *379*, 55.
- Head-Gordon, T.; Hura, G. *Chem. Rev.* **2002**, *102*, 2651.
- Curtiss, L. A.; Blander, M. *Chem. Rev.* **1988**, *88*, 827.
- Liu, K.; Cruzan, J. D.; Saykally, R. *Science* **1995**, *271*, 929.
- Soper, A. K. *Science* **2002**, *297*, 1288.
- Soper, A. K. *Chem. Phys.* **2000**, *258*, 121.
- Badyal, Y. S.; Saboungi, M. L.; Price, D. L.; Shastri, S. D.; Haeflner, D. R.; Soper, A. K. *J. Chem. Phys.* **2000**, *112*, 9206.
- Almenningen, A.; Bastansen, O.; Motzfeldt, T. *Acta Chem. Scand.* **1970**, *24*, 747.
- Madeja, F.; Havenith, M.; Nauta, K.; Miller, R. E.; Chocholousova, J.; Hobza, P. *J. Chem. Phys.* **2004**, *120*, 10554.
- Nahringbauer, I. *Acta Crystallogr.* **1978**, *34*, 315.
- Albinatti, A.; Rouse, K. D.; Thomas, M. W. *Acta Crystallogr.* **1978**, *34*, 2184.
- Chapman, D. *J. Chem. Soc.* **1956**, 225.
- Bartholomew, R. J.; Irish, D. E. *J. Raman Spectrosc.* **1999**, *30*, 325.
- Bertagnolli, H.; Hertz, H. *Ber. Bunsen-Ges. Phys. Chem.* **1985**, *89*, 500.
- Bertagnolli, H.; Chieux, P.; Hertz, H. *Ber. Bunsen-Ges. Phys. Chem.* **1984**, *88*, 977.
- Bako, I.; Schubert, G.; Palinkas, G.; Schwan, G. I.; Dore, J. *Chem. Phys.* **2004**, *306*, 241.
- Gorbunova, T.; Shilov, V. V.; Batalin, G. I. *Russ. J. Struct. Chem.* **1973**, *14*, 424.
- Jedlovsky, P.; Bako, I.; Pálkás, G.; Dore, J. C. *Mol. Phys.* **1995**, *86*, 87.
- Bako, I.; Jedlovsky, P.; Pálkás, G.; Dore, J. C. In *Hydrogen Bonding Liquids* (Proceedings of the NATO ASI Ser C. Vol. 435): Bellissent Funel, M. C., Dore, J. C., Eds.; Kluwer Academic: Dordrecht, 1994; p 119.
- Jedlovsky, P.; Turi, L. *J. Phys. Chem. B.* **1997**, *10*, 2662.
- Mínary, P.; Jedlovsky, P.; Mezei, M.; Turi, L. *J. Phys. Chem. B* **2000**, *104*, 8287.
- Sprk, M.; Hutter, J.; Parrinello, M. *J. Chem. Phys.* **1996**, *105*, 1142.
- VandeVondele, J.; Mohamed, F.; Krack, M.; Hutter, J.; Sprk, M.; Parrinello, M. *J. Chem. Phys.* **2005**, *122*, 1451.
- Asthağiri, D.; Pratt, L. R.; Kress, J. D. *Phys. Rev. E.* **2003**, *68*, 041505.
- Monroe, J. A.; Tuckerman, M. E. *J. Chem. Phys.* **2002**, *117*, 4403.
- Boese, A. D.; Chandra, A.; Martin, J. M. L.; Marx, D. *J. Chem. Phys.* **2003**, *119*, 5965.
- Kreitmer, M.; Bertagnolli, H.; Mortensen, J. J.; Parrinello, M. *J. Chem. Phys.* **2003**, *118*, 3639.
- Kirchner, B.; Hutter, J. *J. Chem. Phys.* **2004**, *121*, 5133.
- Leung, K.; Rempe, S. B. *J. Am. Chem. Soc.* **2004**, *126*, 344.
- Bako, I.; Hutter, J.; Pálkás, G. *J. Chem. Phys.* **2002**, *117*, 9838.
- Lyubatrsev, A. P.; Laasonen, K.; Laaksonen, A. *J. Chem. Phys.* **2001**, *114*, 3120.
- Lighthstone, F. C.; Schwegler, E.; Hood, R. Q.; Gygi, F.; Galli, G. *Chem. Phys. Lett.* **2001**, *343*, 549.
- Lubin, M. I.; Bylaska, J.; Wearm, J. H. *Chem. Phys. Lett.* **2000**, *322*, 447.
- Marx, D.; Sprk, M.; Parrinello, M. *Chem. Phys. Lett.* **1977**, *373*, 360.
- Bempe, S. P.; Pratt, L. *Fluid Phase Equilib.* **2001**, *183–184*, 121.
- Chelli, R.; Righini, R.; Califano, S. *J. Phys. Chem. B.* **2005**, *109*, 17006.
- Becke, A. D. *Phys. Rev. A* **1988**, *38*, 3098.
- Lee, C.; Yang, W.; Parr, R. C. *Phys. Rev. B* **1988**, *37*, 785.
- Troullier, N.; Martins, J. *Phys. Rev. B.* **1991**, *43*, 1993.
- Martyna, G. J.; Tuckerman, M. E. *J. Chem. Phys.* **1999**, *110*, 2810.
- CPMD, Copyright IBM Corp. 1990–2001, Copyright MPI für Festkörperforschung Stuttgart 1997–2001.
- Grossman, J. C.; Schwegler, E.; Draeger, E. W.; Gygi, F.; Galli, G. *J. Chem. Phys.* **2004**, *120*, 300.
- Schwegler, E.; Grossman, J. C.; Draeger, E. W.; Gygi, F.; Galli, G. *J. Chem. Phys.* **2004**, *121*, 5400.
- Tangney, P.; Scandolo, S. *J. Chem. Phys.* **2002**, *116*, 14.
- Fernandez-Serra, M. V.; Artacho, E. *J. Chem. Phys.* **2004**, *121*, 11136.
- Kuo, I. F. W.; Mundy, C. J.; McGrath, M. J.; Siepmann, J. I.; VandeVondele, J.; Sprk, M.; Hutter, J.; Chen, B.; Klein, M. L.; Mohamed, F.; Krack, M.; Parrinello, M. *J. Phys. Chem. B* **2004**, *108*, 12990.
- Császár, A. G.; Allen, W. D.; Schaefer, H. F., III. *J. Chem. Phys.* **1998**, *108*, 9751.
- Chocholousova, J.; Vacek, J.; Hobza, P. *Phys. Chem. Chem. Phys.* **2002**, *4*, 2119.
- Turi, L. *J. Phys. Chem.* **1996**, *100*, 11285.
- Tsuzuki, M.; Uchimaru, T.; Matsumura, K.; Mikami, M.; Tanabe, H. *J. Chem. Phys.* **1999**, *110*, 11906.
- Lim, J. H.; Lee, E. K.; Kim, Y. *J. Phys. Chem. A* **1997**, *101*, 2233.
- Lazaar, K. I.; Bauer, S. H. *J. Am. Chem. Soc.* **1985**, *107*, 3769.
- Henderson, G. *J. Chem. Educ.* **1987**, *64*, 88.
- Hobza, P.; Havlas, Z. *Chem. Rev.* **2000**, *100*, 4253.
- Li, X.; Liu, L.; Schlegel, H. B. *J. Am. Chem. Soc.* **2002**, *124*, 9639.
- Basch, H.; Stevens, W. *J. Am. Chem. Soc.* **1991**, *113*, 95.
- Pan, Y.; McAllister, M. A. *J. Am. Chem. Soc.* **1998**, *120*, 166.
- Smedarchina, Z.; Fernandez-Ramos A.; Siebrand, W. *Chem. Phys. Lett.* **2004**, *395*, 339.
- Markwick, P. R. L.; Doltsinis, N. L.; Marx, D. *J. Chem. Phys.* **2005**, *122*, 054112.
- Tauterman, C. S.; Loferer, M. J.; Voegelé, A. F.; Liedl, K. L. *J. Chem. Phys.* **2004**, *120*, 11650.
- Geiger, A.; Stillinger, F. H.; Rahman, A. *J. Chem. Phys.* **1979**, *79*, 4185.
- Kratochwill, A.; Hertz, H. G. *J. Chim. Phys.* **1977**, *74*, 814.
- Hippler, M. *Phys. Chem. Chem. Phys.* **2002**, *4*, 1457.
- Rapaport, D. C. *Mol. Phys.* **1983**, *50*, 1151.
- Starr, F. W.; Nielsen, J. K.; Stanley, H. E. *Phys. Rev. E.* **2000**, *62*, 579.
- Padro, J. A.; Saiz, L.; Guardia, E. *J. Mol. Struct.* **1997**, *416*, 243.
- Petravic, J.; Delhommelle, J. *J. Chem. Phys.* **2003**, *286*, 303.